

CHEMISTRY

A EUROPEAN JOURNAL

Supporting Information

© Copyright Wiley-VCH Verlag GmbH & Co. KGaA, 69451 Weinheim, 2008

Insights in Sonogashira Cross-Coupling via High-Throughput Kinetics and Descriptor Modelling

Markus an der Heiden,^[a] Herbert Plenio*,^[a] Enrico Burello,^[b] Huub C. J. Hoefsloot,^[c] S. Immel,^[d]] and Gadi Rothenberg,^[b]

[a] Inorganic Chemistry, Zintl-Institute, Darmstadt University of Technology, Petersenstr. 18, D-64287 Darmstadt, Germany; ^[b] van 't Hoff Institute of Molecular Sciences and ^[c] Biosystems Data Analysis, University of Amsterdam, Nieuwe Achtergracht 166, 1018 WV Amsterdam, The Netherlands; ^[d] Organic Chemistry, Schöpf-Institute, Darmstadt University of Technology, Petersenstr. 20, 64287 Darmstadt, Germany

E-mail: plenio@tu-darmstadt.de

List of content -SI

Experimental Section: Synthesis and Gas chromatography

Additional figures and tables

Ligand Geometry Optimization, Descriptors and Statistical Methods

Computational procedures

Sonogashira Coupling Reactions

- a) *Variation of the Aryl Halide (20x1)-screen:* A mixture of the ready-made Sonogashira catalyst (CMIX-1, 20.0 mg) and the respective aryl halide stock solution (500 µL, 0.5 mmol) in HNiPr₂ (4.5 mL) was carefully degassed (freeze and thaw) and then heated to a given temperature with vigorous stirring for 10 minutes. The concentration for the aryl halides at the beginning of the reaction is 0.1M. Initiation of reaction is done by the addition of the phenylacetylene (150 µL, 1.37 mmol), the precipitation of HNiPr₂·HBr indicates the start of the reaction and stirring was continued until full conversion. GC samples were taken at given times and stored as described above.
- b) *Sequential variation of the Phosphines – the different Catalyst Mixtures:* The catalyst component mixtures (palladium-, copper- and the respective phosphine-composition CMIX2-P(a-s)), in each case are weighed in a schlenk tube (each: 5.0 mg). This mixture and the respective aryl halide stock solution (500 µL, 0.5 mmol, see chapter 0) in HNiPr₂ (4.5 mL) was carefully degassed (freeze and thaw) and then heated to 80°C with vigorous stirring for 10 minutes. The concentration for the aryl halides at the beginning of the reaction is 0.1M. Initiation of reaction is done by the addition of the phenyl acetylene (150 µL, 1.37 mmol), the precipitation of HNiPr₂·HBr indicates the start of the reaction and stirring was continued until full conversion. GC samples were taken at given times and stored as described above..

Additional figures and tables

	<i>n</i> Bu ₃ P	Cy ₂ PBn	PCy ₃	<i>i</i> Pr ₂ PCy ₂	<i>i</i> Pr ₃ P	<i>sec</i> Bu ₃ P	(1-Ad)PCy ₂	<i>t</i> BuPCy ₂	<i>t</i> BuPiPr ₂	(1-Ad) ₂ PEt	<i>t</i> Bu ₂ PCy	<i>t</i> Bu ₂ PiPr	<i>t</i> Bu ₃ P	<i>t</i> Bu ₂ PBn	(1-Ad) ₂ PBn	(1-Ad) ₂ PBu	
p-NO ₂	0,175	1,346	3,584	4,210	6,111	5,941	8,491	10,05	20,67	21,83	20,18	23,62	30,96	30,57	32,44	34,96	46,36
p-CN	0,112	0,790	2,247	2,323	3,401	3,667	5,524	9,218	11,63	10,32	12,46	13,52	16,62	21,04	20,69	24,42	26,49
m-SOMe	0,030	0,549	0,660	0,738	0,775	1,241	2,072	4,420	4,641	5,366	7,548	6,704	12,68	10,59	19,58	25,51	21,78
p-SOMe	0,029	0,226	0,894	0,571	0,420	1,341	1,844	5,311	3,990	3,827	8,619	5,467	14,27	9,810	9,942	14,38	15,76
p-COMe	0,048	0,373	0,982	1,148	1,738	1,782	3,073	6,136	6,411	6,142	8,953	7,400	8,842	13,04	13,13	17,21	16,33
m-COMe	0,019	0,204	0,618	0,576	0,842	0,957	1,696	4,109	3,754	3,625	6,095	4,556	6,138	9,588	8,733	11,36	13,97
p-CO ₂ Et	0,035	0,288	0,848	0,875	1,171	1,303	2,428	5,074	4,659	4,307	6,863	4,604	6,098	8,510	8,763	10,81	10,97
m-CO ₂ Et	0,016	0,123	0,475	0,400	0,602	0,695	1,828	3,410	2,785	2,778	4,266	3,114	4,328	4,635	6,555	8,448	10,58
m-CF ₃	0,027	0,284	0,961	0,982	1,234	1,394	1,710	4,961	5,653	4,370	5,085	6,021	6,746	8,891	9,354	10,81	9,046
p-CF ₃	0,042	0,291	0,824	0,828	1,092	1,314	1,819	4,144	3,859	3,677	4,731	3,454	4,212	6,843	7,164	8,673	6,050
m-F	0,017	0,125	0,283	0,339	0,390	0,505	0,801	1,619	1,823	1,896	2,004	1,712	2,589	3,853	4,070	4,868	3,727
p-F	0,006	0,069	0,150	0,166	0,195	0,306	0,474	0,937	1,238	1,190	1,275	1,242	1,533	2,790	3,187	3,759	3,418
H	0,014	0,094	0,169	0,192	0,182	0,350	0,609	1,361	1,181	1,143	1,593	1,354	2,156	3,347	3,494	4,022	3,411
m-Me	0,006	0,071	0,146	0,145	0,178	0,249	0,415	0,845	0,940	0,988	1,215	0,952	1,186	2,390	2,609	3,146	2,383
p-Me	0,005	0,062	0,122	0,155	0,116	0,230	0,339	0,761	0,724	0,722	1,041	0,832	1,230	2,035	2,180	2,708	1,895
m-OMe	0,008	0,072	0,178	0,197	0,211	0,306	0,491	1,099	1,078	1,110	1,452	1,092	1,633	2,773	2,888	3,587	2,930
p-OMe	0,006	0,047	0,112	0,121	0,166	0,183	0,351	0,317	0,755	0,804	0,843	0,866	1,194	1,920	2,071	2,724	3,029
p-tBu	0,005	0,039	0,084	0,224	0,106	0,155	0,185	0,640	0,948	0,758	0,900	0,668	1,160	1,583	1,836	2,550	1,272
m-NMe ₂	0,004	0,056	0,135	0,178	0,132	0,200	0,358	0,635	0,864	0,548	1,299	0,856	1,157	2,366	2,653	3,297	2,346
p-NMe ₂	0,002	0,026	0,066	0,076	0,070	0,082	0,256	0,480	0,821	0,283	0,930	0,966	0,697	1,729	1,076	0,896	2,479

Table 1: First-order rate constants for 340 Sonogashira reactions of 20 aryl bromides with phenyl acetylene, applying 17 different Pd-phosphine complexes. [1000/h⁻¹] Solvent: HN*i*Pr₂, T= 80°C, Catalyst: Na₂PdCl₄, CuI, phosphonium salt: 4: 3: 4.

	S_{para}^θ	S_{para}^-	S_{para}^+	F	R	R^-	R^+	S_{meta}^θ
-H	0	0	0	0	0	0	0	0
-CF₃	0.54	0.65	0.61	0.38	0.16	0.27	0.23	0.43
-Me	-0.17	-0.17	-0.31	0.01	-0.18	-0.18	-0.32	-0.07
-CN	0.66	1	0.66	0.51	0.15	0.49	0.15	0.56
-CO₂R	0.45	0.75	0.48	0.34	0.11	0.41	0.14	0.37
-COMe	0.5	0.84		0.33	0.17	0.51		0.38
-F	0.06	-0.03	-0.07	0.45	-0.39	-0.48	-0.52	0.34
-NMe₂	-0.83	-0.12	-1.7	0.15	-0.98	-0.27	-1.85	-0.16
-NO₂	0.78	1.27	0.79	0.65	0.13	0.62	0.14	0.71
-OMe	-0.27	-0.26	-0.78	0.29	-0.56	-0.55	-1.07	0.12
-SOMe	0.49	0.73		0.52	-0.03	0.21		0.52

Table 2: List of Hammett constants used.

	X = Cl		X = Br		X = I	
	[kJ·mol ⁻¹]		[kJ·mol ⁻¹]		[kJ·mol ⁻¹]	
NO₂	94,5	± 4,8	53,5	± 4,4	47,7	± 2,9
CO₂Et	113,2	± 5,8	61,4	± 5,1	56,4	± 2,9
CF₃	111,1	± 5,7	61,7	± 3,3	58,6	± 2,9
H	117,1	± 6,0	73,6	± 3,8	61,6	± 3,1
F	118,6	± 6,0	72,9	± 3,8	62,0	± 3,1
CH₃	140,8	± 7,1	78,9	± 4,0	62,1	± 3,1
OMe	143,7	± 7,2	81,9	± 4,3	61,6	± 3,1

Table 3: Activation enthalpy DH^\ddagger .

	$X = Cl$		$X = Br$		$X = I$	
	[J·mol⁻¹K⁻¹]		[J·mol⁻¹K⁻¹]		[J·mol⁻¹K⁻¹]	
NO₂	-6,3	± 10	-86,4	± 12	-64,8	± 8
CO₂Et	40,7	± 12	-39,9	± 13	-49,1	± 7
CF₃	36,3	± 12	-41,8	± 8	-42,9	± 8
H	34,8	± 12	-10,4	± 10	-37,8	± 8
F	36,1	± 12	-13,4	± 9	-36,5	± 8
CH₃	96,6	± 15	1,3	± 10	-37,4	± 8
OMe	99,9	± 15	10,5	± 11	-38,5	± 8

Table 4: Activation entropy DS^\ddagger .

	Temperature	Product formation rate [h⁻¹]						
		NO₂	CO₂Et	CF₃	H	F	Me	OMe
X=ArI	23.4°C	4.6	2.3	1.8	1.01	0.99	0.87	0.95
	30°C	6.9	3.8	2.8	1.62	1.59	1.35	1.39
	35°C	9.1	5.0	4.2	2.1	2.1	1.8	1.9
	40°C	14.1	6.7	5.7	3.3	3.2	2.8	2.9
	45°C	17.6	9.3	7.5	4.7	4.6	4.0	4.2
	50°C	24.8	11.5	9.9	6.1	6.0	5.3	5.6
X=Ar-Br	40°C	17.2	3.2	2.1	0.95	0.95	0.52	0.48
	50°C	21.7	6.4	4.1	2.2	2.0	1.2	1.2
	60°C	35.6	10.6	7.1	4.3	3.9	2.6	2.7
	70°C	59.0	21.1	13.9	9.9	8.8	6.5	6.8
	80°C	125.6	50.2	28.4	23.6	21.4	17.1	17.8
X=Ar-Cl	80°C	$3.6 \cdot 10^{-2}$	$1.5 \cdot 10^{-2}$	$1.7 \cdot 10^{-2}$	$1.7 \cdot 10^{-3}$	$1.2 \cdot 10^{-3}$	$9 \cdot 10^{-4}$	$5 \cdot 10^{-4}$
	95°C	$13.8 \cdot 10^{-2}$	$7.0 \cdot 10^{-2}$	$7.8 \cdot 10^{-2}$	$8.7 \cdot 10^{-3}$	$5.7 \cdot 10^{-3}$	$6.4 \cdot 10^{-3}$	$3.7 \cdot 10^{-3}$
	108°C	0.59	0.39	0.44	$5.0 \cdot 10^{-2}$	$2.9 \cdot 10^{-2}$	$5.3 \cdot 10^{-2}$	$2.6 \cdot 10^{-2}$

Table 5: First-order rate constants for the Sonogashira coupling of aryl chlorides, - bromides and -iodides at different temperatures. [1000/h⁻¹]. Catalysts concentration in chloroarene screen was 10 mol%.

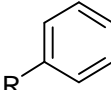
	Temperature		Reaction constant <i>r</i>			
	[°C]	<i>r</i> (σ^-)	<i>R</i>	<i>r</i> (σ^0)	<i>R</i>	
I -	23.4	0.457	0.97	0.635	0.87	
I -	30	0.461	0.98	0.646	0.90	
I -	35	0.459	0.99	0.647	0.92	
I -	40	0.445	0.97	0.624	0.89	
I -	45	0.408	0.97	0.57	0.89	
I -	50	0.376	0.98	0.527	0.90	
Br -	40	0.921	0.95	1.302	0.89	
Br -	50	0.762	0.96	1.077	0.90	
Br -	60	0.675	0.95	0.946	0.87	
Br -	70	0.568	0.93	0.79	0.84	
Br -	80	0.508	0.89	0.693	0.77	
Cl -	80	1.336	0.98	1.955	0.98	
Cl -	95	1.097	0.95	1.603	0.94	
Cl -	108	0.98	0.90	1.42	0.88	

Table 6. Full listing of hammett correlations for the temperature-variable Sonogashira reactions of Ar-X (X= Cl, Br, I). Comparison of σ^- and σ^0 correlations.

Ad ₂ PtBu	190
Ad ₂ PiPr	182.7
tBu ₃ P	182
tBu ₂ PCy	178
tBu ₂ PiPr	174.7
Ad ₂ PBn	174.7
tBuPCy ₂	174
Ad ₂ PEt	173.3
PCy ₃	170
tBuPiPr ₂	167.3
iPrPCy ₂	166.7
tBu ₂ PBn	166.7
iPr ₂ PCy	163.3
secBu ₃ P	163
iPr ₃ P	160
Cy ₂ PBn	158.7
nBu ₃ P	132

Table 7. Tolman cone angles for the phosphines used in this study, calculated according to Tolman, *Chem. Rev.* **1977**, 77, 313.

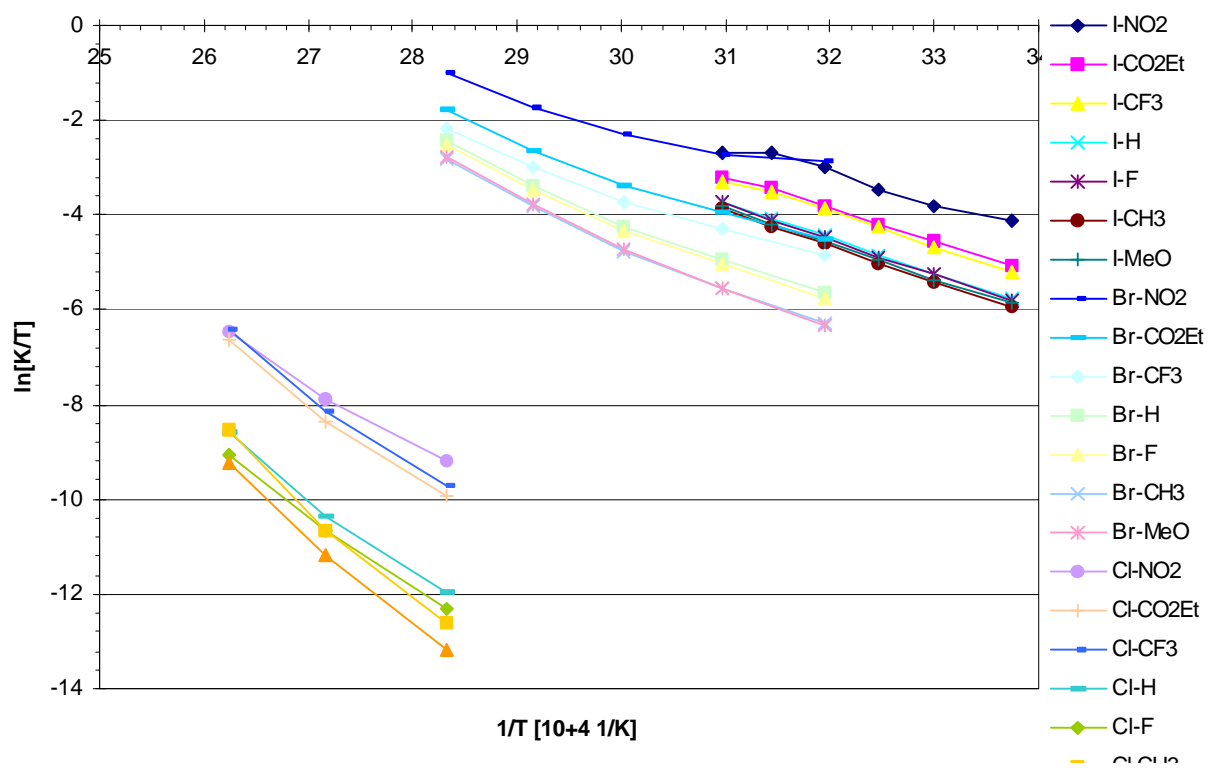


Figure 8. Eyring plot for the Sonogashira coupling of aryl chlorides, -bromides and -iodides

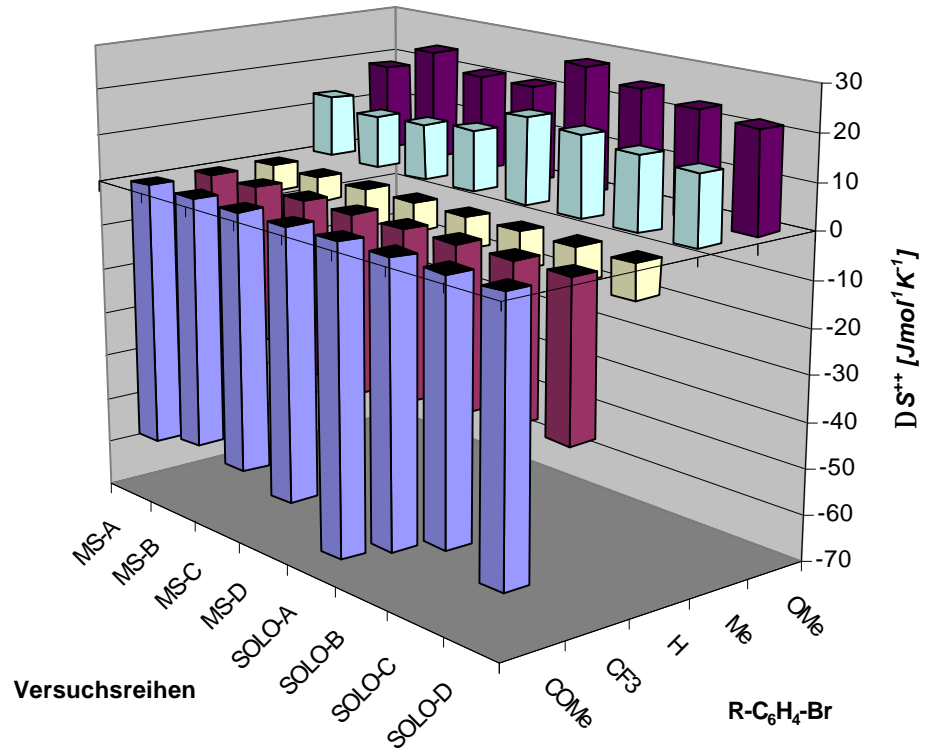
	MS-A [J·mol ⁻¹ ·K ⁻¹]	MS-B [J·mol ⁻¹ ·K ⁻¹]	MS-C [J·mol ⁻¹ ·K ⁻¹]	MS-D [J·mol ⁻¹ ·K ⁻¹]	Mittelwert [J·mol ⁻¹ ·K ⁻¹]
COMe	-58,0 ± 11	-55,0 ± 11	-56,6 ± 11	-59,0 ± 11	-57,2 ± 11
CF₃	-35,4 ± 12	-34,2 ± 12	-38,6 ± 11	-39,0 ± 11	-36,9 ± 11
H	-6,0 ± 7	-5,6 ± 7	-8,1 ± 7	-6,3 ± 7	-6,5 ± 7
Me	13,4 ± 15	11,5 ± 15	12,1 ± 14	13,4 ± 14	12,6 ± 15
OMe	18,5 ± 17	24,2 ± 18	20,9 ± 17	21,0 ± 17	21,1 ± 17

Tabelle 9a: Activation entropy ΔS^\ddagger MS-5 multisubstrate screening.

	SOLO-A [J·mol ⁻¹ ·K ⁻¹]	SOLO-B [J·mol ⁻¹ ·K ⁻¹]	SOLO-C [J·mol ⁻¹ ·K ⁻¹]	SOLO-D [J·mol ⁻¹ ·K ⁻¹]	Mittelwert [J·mol ⁻¹ ·K ⁻¹]
COMe	-66,8 ± 11	-60,3 ± 11	-55,1 ± 11	-58,9 ± 11	-60,1 ± 11
CF₃	-36,5 ± 12	-35,1 ± 12	-33,2 ± 12	-33,2 ± 12	-34,4 ± 12
H	-6,9 ± 7	-7,9 ± 7	-7,3 ± 7	-7,7 ± 7	-7,5 ± 7
Me	18,6 ± 15	17,6 ± 15	16,1 ± 14	15,2 ± 14	17,0 ± 14
OMe	27,6 ± 17	25,0 ± 17	23,3 ± 17	21,8 ± 17	24,6 ± 17

Tabelle 9b: Activation entropy ΔS^\ddagger from the single reaction experiments.

Aktivierungsentropie alle Reihen



Verification Screens Eyring Plots

Table 10

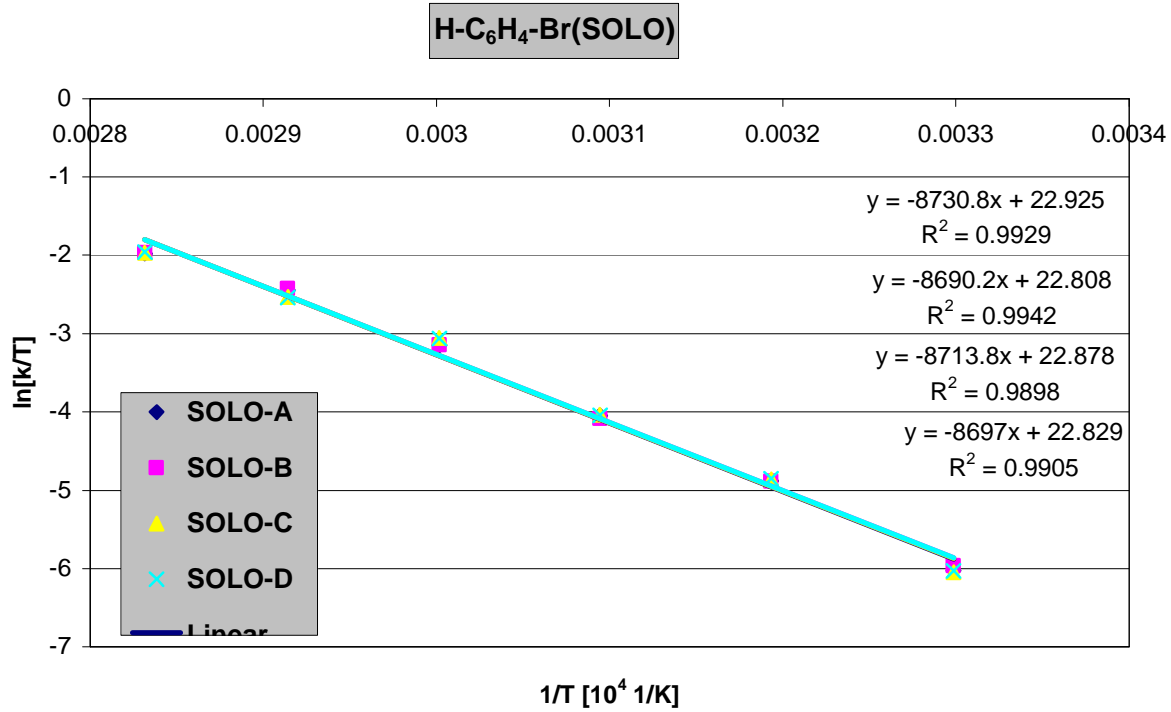
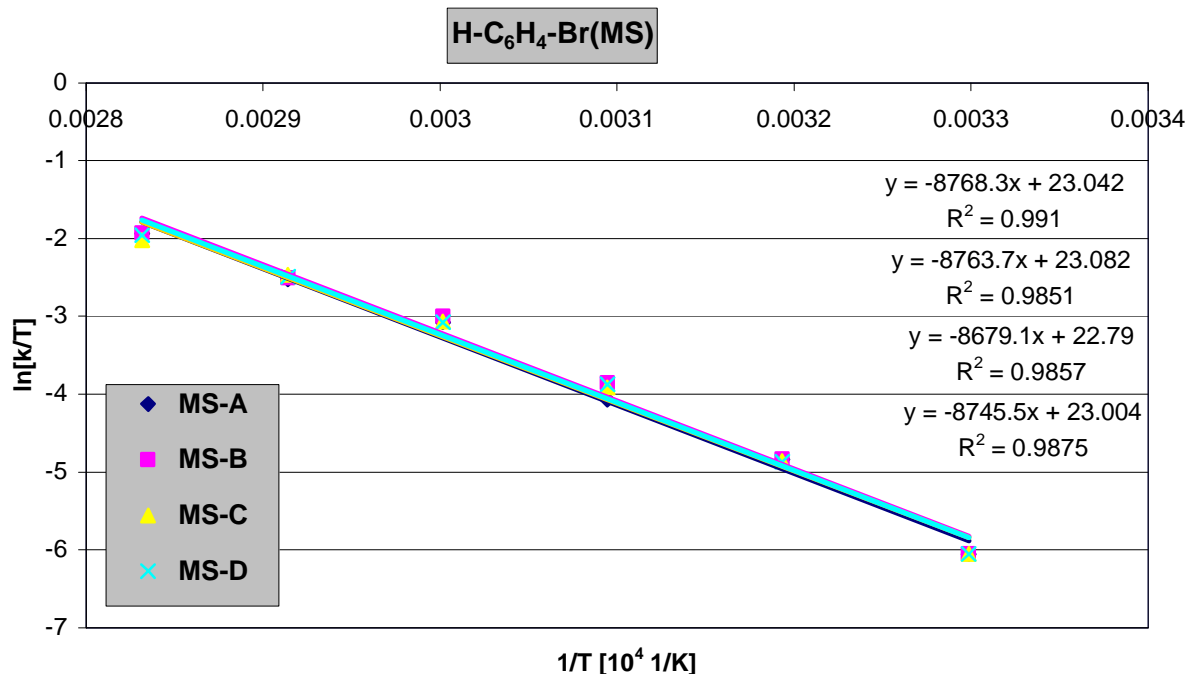


Table 11



R-C₆H₄-Br(MS)

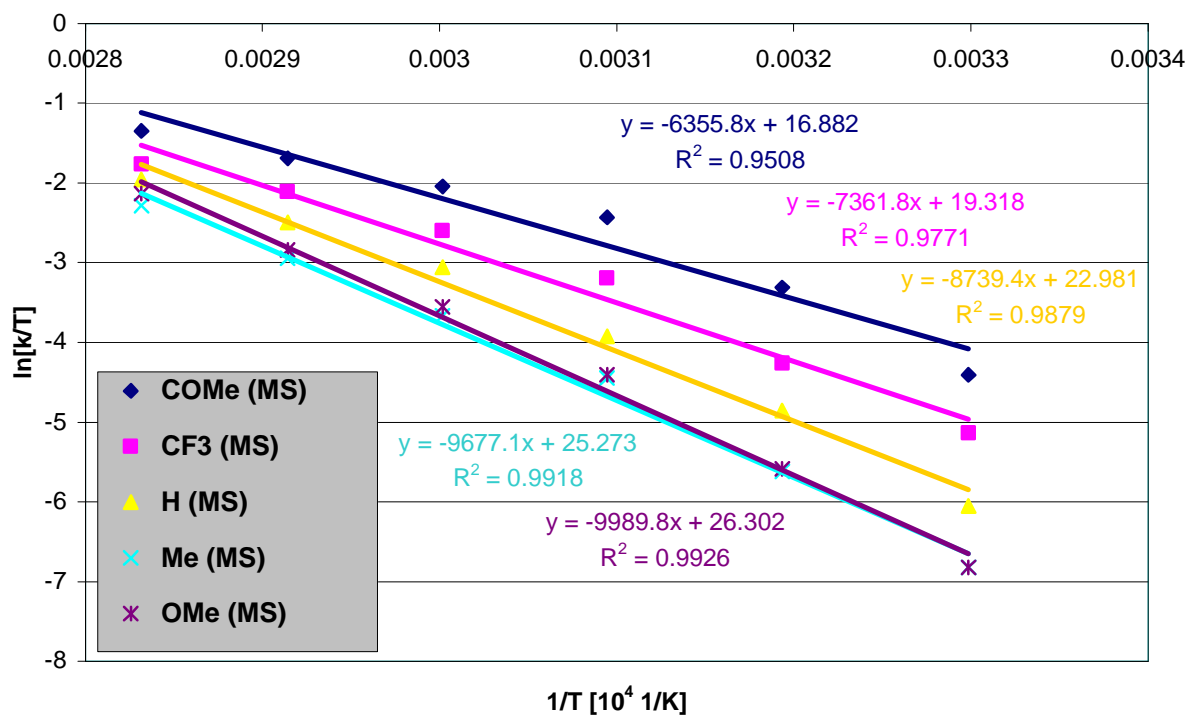
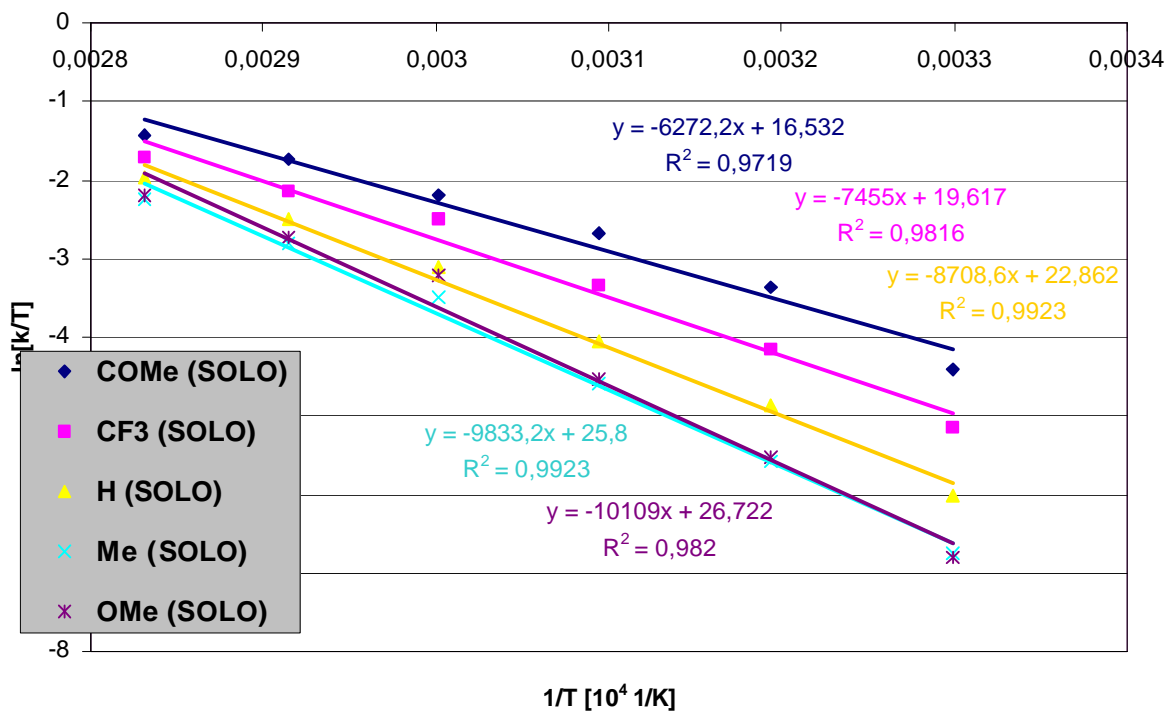


Table 12

R-C₆H₄-Br(SOLO)



Ligand Geometry Optimization, Descriptors And Statistical Methods

Computational methods. Statistical analyses were performed using the Statistica Software. PCA and linear regression analysis methods were described elsewhere.^[1]

References:

1. Burello E.; Rothenberg, G. “Combinatorial Explosion in Homogeneous Catalysis: Screening 60,000 Cross-Coupling Reactions” *Adv. Synth. Catal.*, **2004**, 346, 1844–1853.

Computational procedures DFT Calculations

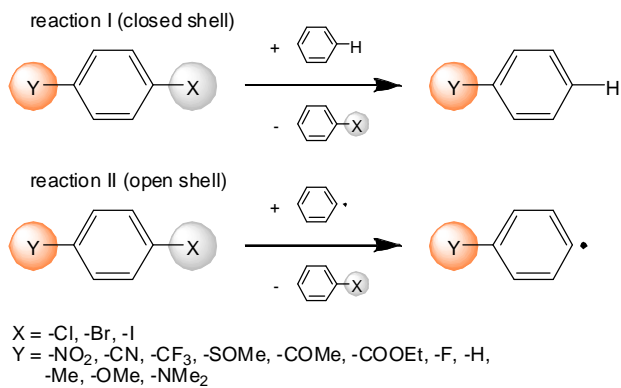
All calculations were performed on AMD Opteron® 846 based 64-bit LINUX computer systems of the Frankfurt Center for Scientific Computing. All DFT (B3LYP^[1,2]). Computations were carried out using the Gaussian03^[3] suite of programs, all structure setups, analysis protocols, and molecular graphics were prepared using the MolArch⁺ utility.^[4] All structures were pre-optimized at the B3LYP/6-311G(d) level of theory, and then fully refined with tight optimization criteria and ultrafine DFT grids using the 6-311++G(d,p) basis set^[5] with added diffuse and polarization functions; the halogen atoms Cl, Br, and I were represented by Los Alamos LanL2DZ^[7] effective core potentials (ECPs). Unscaled frequencies were used to calculate zero-point energies (ZPEs) and the thermal corrections needed for the ΔH and ΔG values, as well as to unequivocally establish the true energy minimum nature of all structures. In the case of the aryl radicals (UB3LYP), the spin expectation value of $\langle \hat{S}^2 \rangle$ did not exceed 0.7578 before annihilation, and was reduced to exactly 0.7500 after annihilation in all cases. Molecular orbital energies were derived from the DFT derived Kohn-Sham orbitals except for the E_{HOMO} of *p*-acetyl chlorobenzene and the *p*-methylsulfinyl substituted aryl halogenides (X = -Cl, -Br, and -I), for which the highest occupied MO corresponds to the free electron pair of the carbonyl group and the sulfur atom, respectively. In these cases – after visual inspection of the MOs – the energies of the next lower occupied orbital of appropriate symmetry (HOMO-1) were used.

References

- [1] Density-functional exchange-energy approximation with correct asymptotic behavior: A. D. Becke, *Phys. Rev. A* **1988**, 38, 3098-3100; Density-functional thermochemistry. III. The role of exact exchange: A. D. Becke, *J. Chem. Phys.* **1993**, 98, 5648-5652.
- [2] Development of the Colle-Salvetti correlation-energy formula into a functional of the electron density: C. Lee, W. Yang, R. G. Parr, *Phys. Rev. B* **1988**, 37, 785-789; Results obtained with the correlation energy density functionals of Becke and Lee, Yang and Parr: B. Miehlich, A. Savin, H. Stoll, H. Preuss, *Chem. Phys. Lett.* **1989**, 157, 200-206.
- [3] M. J. Frisch, G. W. Trucks, H. B. Schlegel, G. E. Scuseria, M. A. Robb, J. R. Cheeseman, J. A. M. Jr., T. Vreven, K. N. Kudin, J. C. Burant, J. M. Millam, S. S. Iyengar, J. Tomasi, V. Barone, B. Mennucci, M. Cossi, G. Scalmani, N. Rega, G. A. Petersson, H. Nakatsuji, M. Hada, M. Ehara, K. Toyota, R. Fukuda, J. Hasegawa, M.

Ishida, T. Nakajima, Y. Honda, O. Kitao, H. Nakai, M. Klene, X. Li, J. E. Knox, H. P. Hratchian, J. B. Cross, V. Bakken, C. Adamo, J. Jaramillo, R. Gomperts, R. E. Stratmann, O. Yazyev, A. J. Austin, R. Cammi, C. Pomelli, J. W. Ochterski, P. Y. Ayala, K. Morokuma, G. A. Voth, P. Salvador, J. J. Dannenberg, V. G. Zakrzewski, S. Dapprich, A. D. Daniels, M. C. Strain, O. Farkas, D. K. Malick, A. D. Rabuck, K. Raghavachari, J. B. Foresman, J. V. Ortiz, Q. Cui, A. G. Baboul, S. Clifford, J. Cioslowski, B. B. Stefanov, G. Liu, A. Liashenko, P. Piskorz, I. Komaromi, R. L. Martin, D. J. Fox, T. Keith, M. A. Al-Laham, C. Y. Peng, A. Nanayakkara, M. Challacombe, P. M. W. Gill, B. Johnson, W. Chen, M. W. Wong, C. Gonzalez, J. A. Pople, *Gaussian 03, Revision C.02 - Electronic Structure Program*, Gaussian, Inc., Wallingford CT, **2004**.

- [4] S. Immel, *MolArch⁺ - MOlecular ARCHitecture Modeling Program v8.00*, Technical University of Darmstadt, Germany, **2006**.
- [5] Self-consistent molecular orbital methods. XX. A basis set for correlated wave functions: R. Krishnan, J. S. Binkley, R. Seeger, J. A. Pople, *J. Chem. Phys.* **1980**, 72, 650-654; Contracted Gaussian basis sets for molecular calculations. I. Second row atoms, Z=11--18: A. D. McLean, G. S. Chandler, *J. Chem. Phys.* **1980**, 72, 5639-5648.
- [6] Ab initio effective core potentials for molecular calculations. Potentials for main group elements Na to Bi: W. R. Wadt, P. J. Hay, *J. Chem. Phys.* **1985**, 82, 284-298.



Scheme 1. Isodesmic reactions type I and II for evaluating substituent effects on aryl-halogen bond energies of various *para*-substituted (Y) halogen benzenes (X) relative to their unsubstituted counterparts (Y = -H).

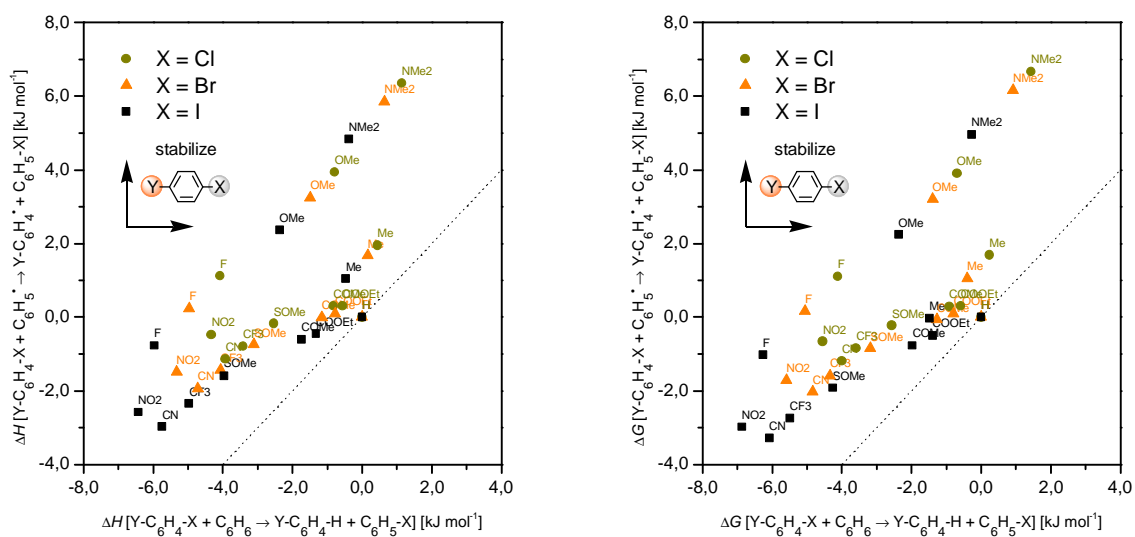


Fig. 1. Correlation of aryl-halogen bond energies (left: $\Delta\Delta H$, right: $\Delta\Delta G$; all energies in kJ mol^{-1} relative to $Y = -\text{H}$) as derived from the isodesmic reactions type I and II (cf. Scheme 1; B3LYP/6-311++G(d,p) with LANL2DZ ECP on $X = -\text{Cl}, -\text{Br}$, and $-I$). For $X = -\text{Br}$, the closed shell reaction of type I finds the stability (based on $\Delta\Delta H$) of the aryl-halogen bond to increase in the order $Y = -\text{NO}_2 < -\text{F} < -\text{CN} < -\text{CF}_3 < -\text{SOMe} < -\text{OMe} < -\text{COMe} < -\text{COOEt} < -\text{H} < -\text{Me} < -\text{NMe}_2$. In contrast, the radical type reaction II indicates the stability of the Ar-Br bond in the order $Y = -\text{CN} < -\text{NO}_2 \approx -\text{CF}_3 < -\text{SOMe} < -\text{COMe} \approx -\text{H} \approx -\text{COOEt} < -\text{F} < -\text{Me} < -\text{OMe} < -\text{NMe}_2$ (order varies only slightly for $X = -\text{Cl}$ or $-I$, or for the corresponding $\Delta\Delta G$ values).

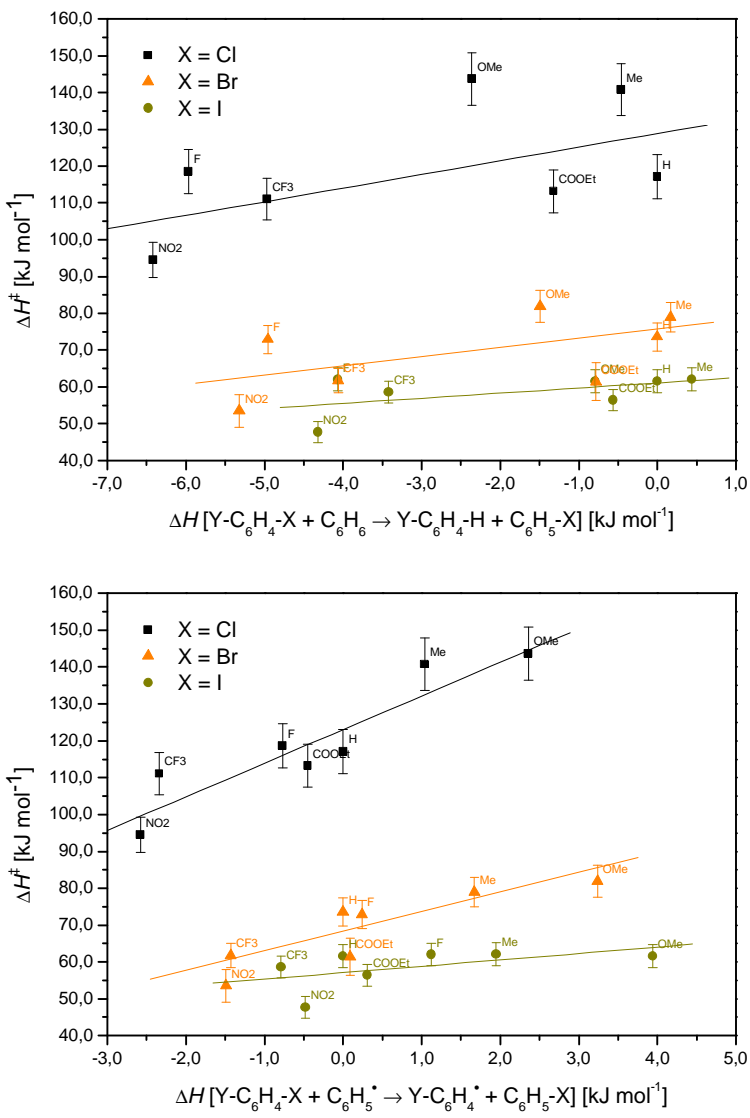


Fig. 2. Relationship between the calculated (B3LYP/6-311++G(d,p) with LANL2DZ ECP on X = -Cl, -Br, and -I) relative aryl-halogen bond energies $\Delta\Delta H$ (top: isodesmic reaction of type I, bottom: reaction of type II cf. Scheme 1; all energies in kJ mol^{-1} relative to Y = -H) and the experimental enthalpies of activation ΔH^\ddagger for the Sonogashira cross-coupling reaction of various substituted (Y = $-\text{NO}_2$, $-\text{CF}_3$, $-\text{COOEt}$, $-\text{F}$, $-\text{H}$, $-\text{Me}$, and $-\text{OMe}$) aryl halogenides (X = -Cl, -Br, and -I).

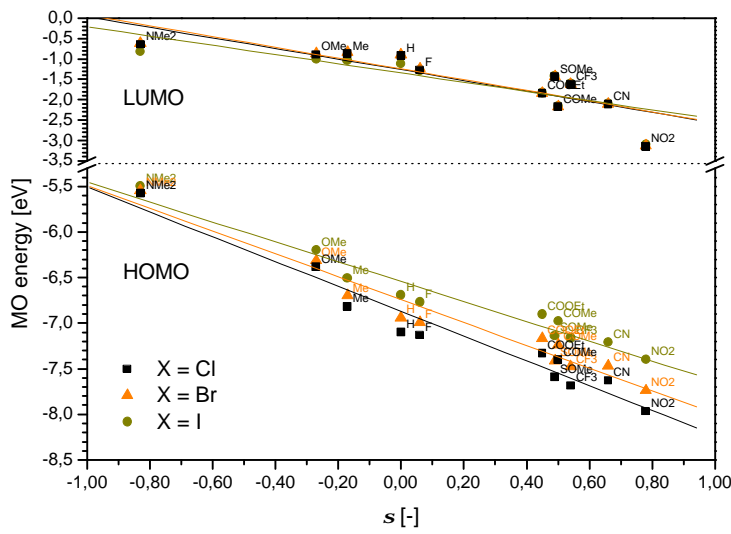


Fig. 3a. Linear least-squares fit correlation of Kohn-Sham MO energies (HOMO and LUMO) with Hammett s -parameters as calculated for a series of substituted aryl halogenides (B3LYP/6-311++G(d,p) with LANL2DZ ECP on X = -Cl, -Br, and -I).

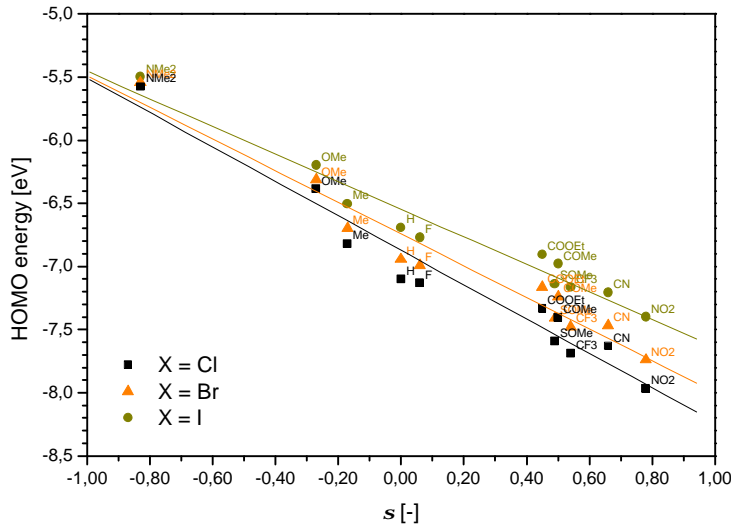


Fig. 3b. Linear least-squares fit correlation of Kohn-Sham HOMO energies with Hammett s -parameters as calculated for a series of substituted aryl halogenides (B3LYP/6-311++G(d,p) with LANL2DZ ECP on X = -Cl, -Br, and -I).

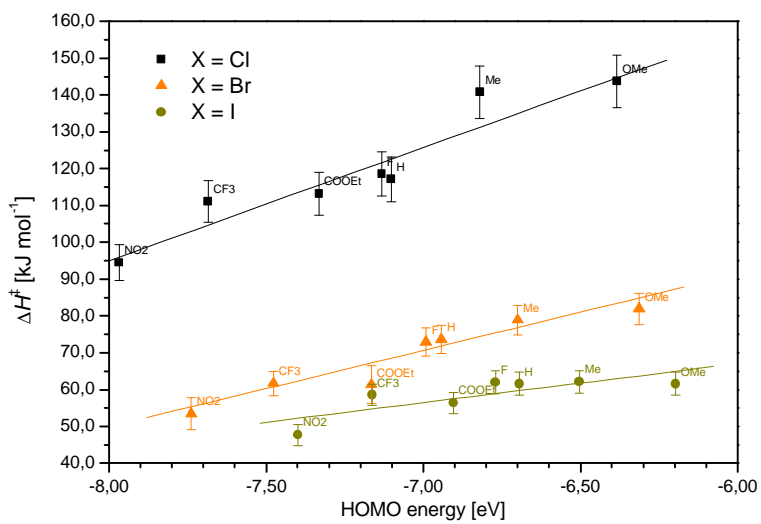
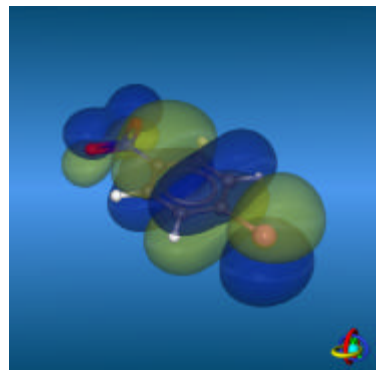
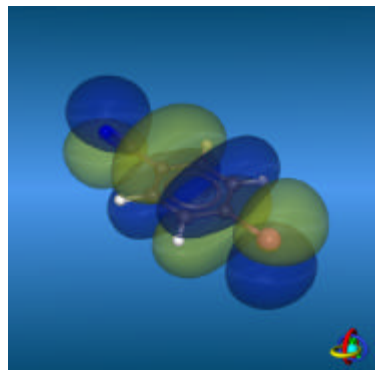


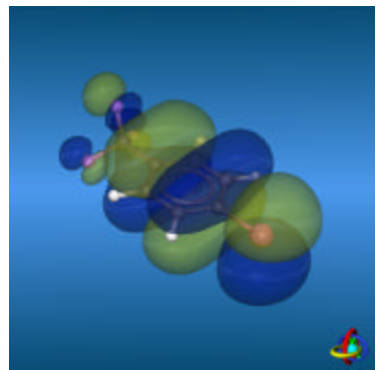
Fig. 4. Plot of experimental enthalpies of activation ΔH^\ddagger against calculated Kohn-Sham HOMO energies for the series of substituted aryl halogenides ($X = -\text{Cl}$, $-\text{Br}$, and $-\text{I}$) used in this kinetic study of the Sonogashira reaction (error weighted linear least-squares fit).



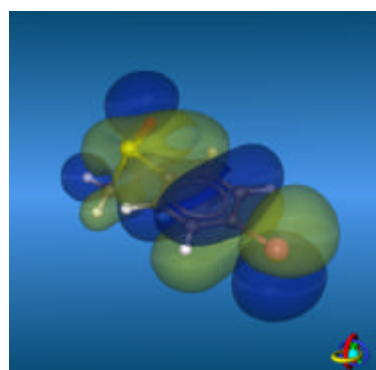
$\text{Y} = \text{-NO}_2$ (-7,967)



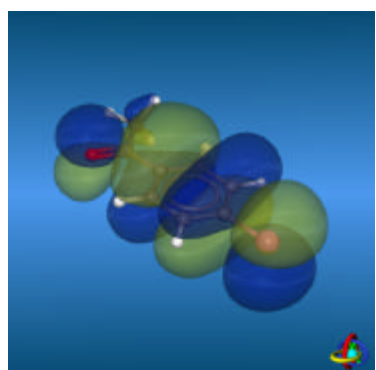
$\text{Y} = \text{-CN}$ (-7,630)



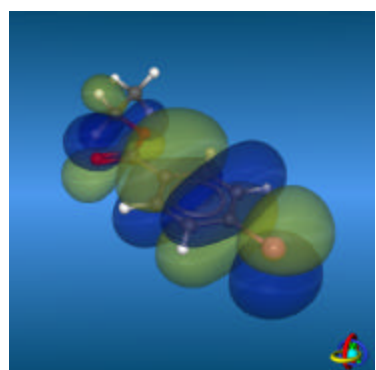
$\text{Y} = \text{-CF}_3$ (-7,685)



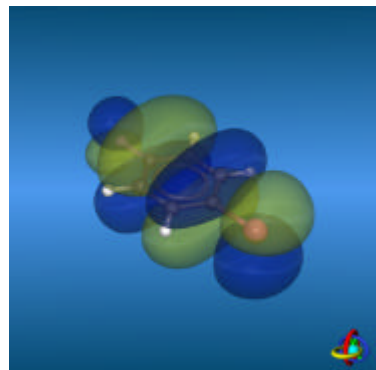
$\text{Y} = \text{-SOMe}$ (-7,593)



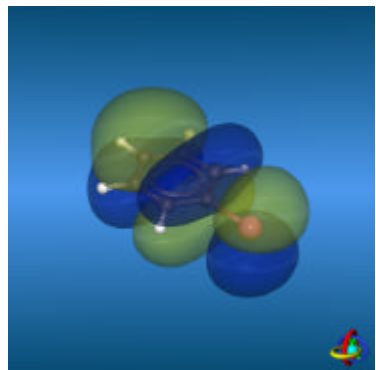
$\text{Y} = \text{-COMe}$ (-7,404)



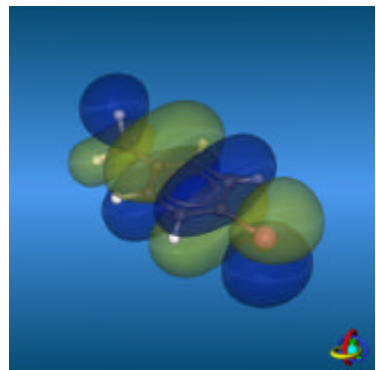
$\text{Y} = \text{-COOEt}$ (-7,332)



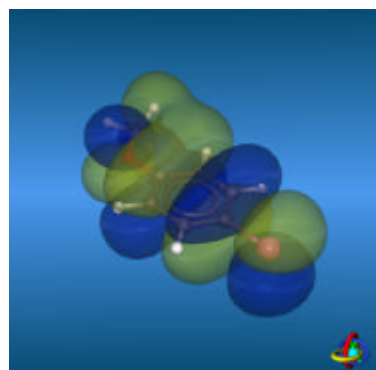
$\text{Y} = \text{-F}$ (-7,132)



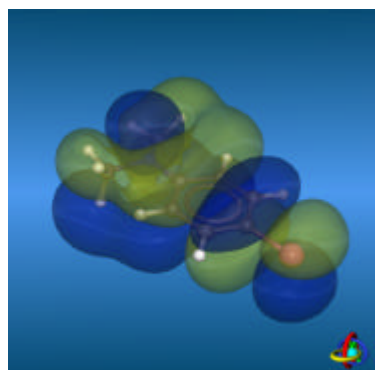
$\text{Y} = \text{-H}$ (-7,102)



$\text{Y} = \text{-Me}$ (-6,820)

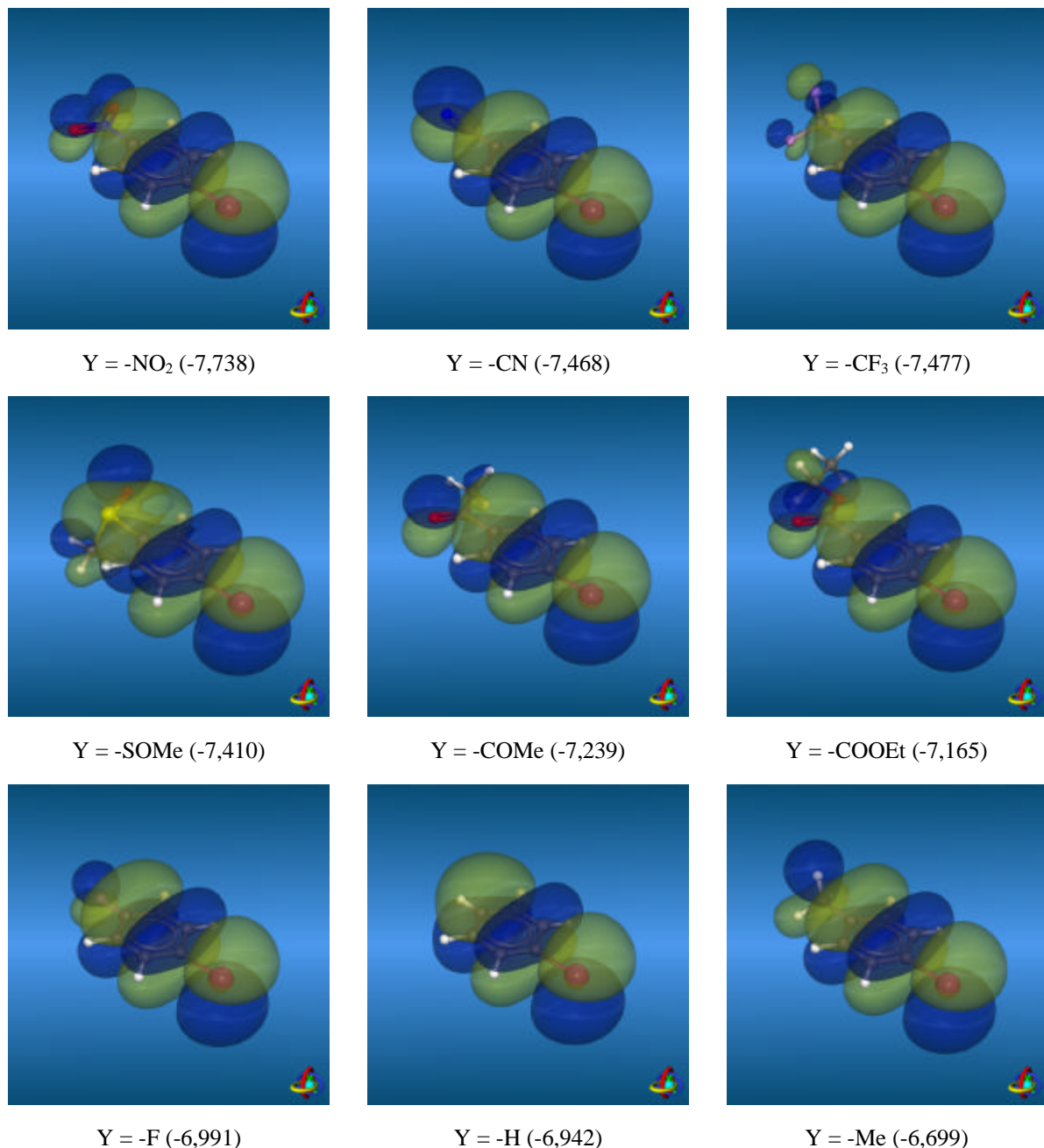


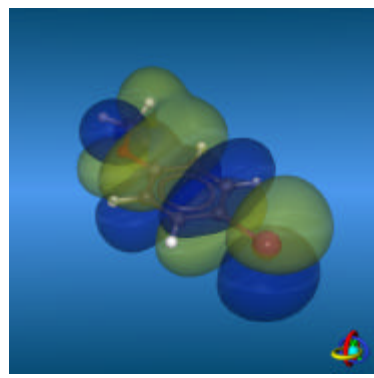
$\text{Y} = \text{-OMe}$ (-6,384)



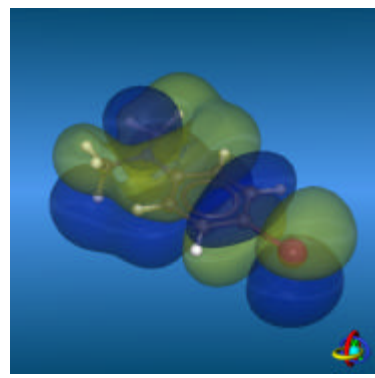
$\text{Y} = \text{-NMe}_2$ (-5,577)

Fig. 5. Highest occupied Kohn-Sham orbitals (HOMOs, B3LYP/6-311++G(d,p) with LANL2DZ ECP on Br, 99% probability contour plots with yellow and blue colors indicating opposite sign of the wave function, all energies in eV) for *para*-substituted chloro-benzenes ($X = -\text{Cl}$). Note that for $Y = -\text{SOMe}$ and $-\text{COMe}$ the HOMO (-6,726 and -7,355eV, resp.) mostly represent the free electron pair located at the sulfur atom or the carbonyl group, and therefore, were replaced by the HOMO-1 (-7,593 and -7,404eV) in the above plots.



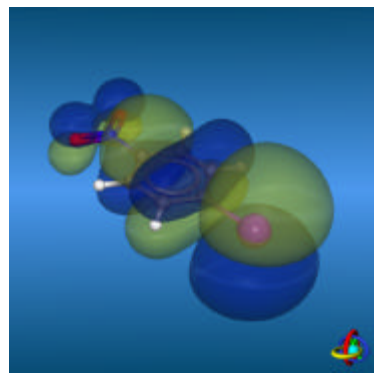


$Y = -\text{OMe}$ (-6,313)

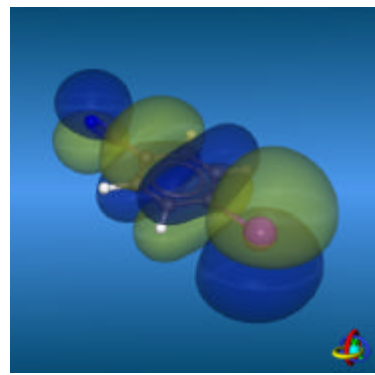


$Y = -\text{NMe}_2$ (-5,545)

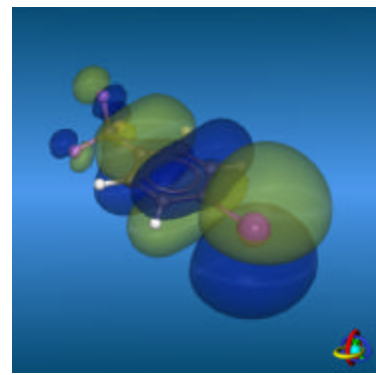
Fig. 6. Highest occupied Kohn-Sham orbitals (HOMOs, B3LYP/6-311++G(d,p) with LANL2DZ ECP on Br, 99% probability contour plots with yellow and blue colors indicating opposite sign of the wave function, all energies in eV) for *para*-substituted bromo-benzenes ($X = -\text{Br}$). Note that for $Y = -\text{SOMe}$ the HOMO (-6,694eV) mostly represents the free electron pair located at the sulfur atom, and therefore, was replaced by the HOMO-1 (-7,410eV) in the above plots.



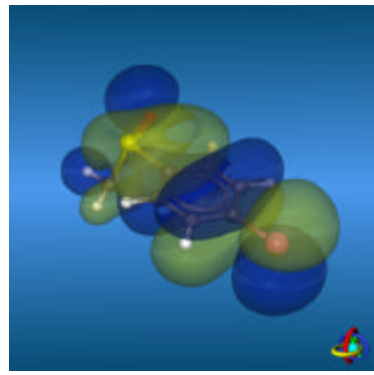
$Y = -\text{NO}_2$ (-7,399)



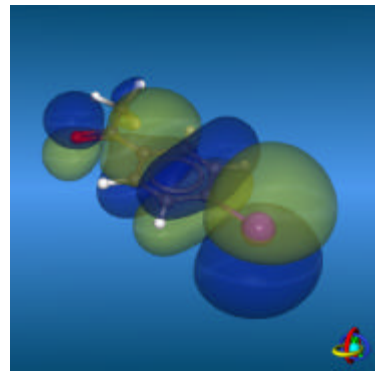
$Y = -\text{CN}$ (-7,207)



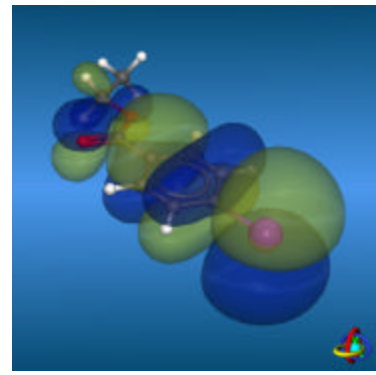
$Y = -\text{CF}_3$ (-7,163)



$Y = -\text{SOMe}$ (-7,138)



$Y = -\text{COMe}$ (-6,978)



$Y = -\text{COOEt}$ (-6,904)

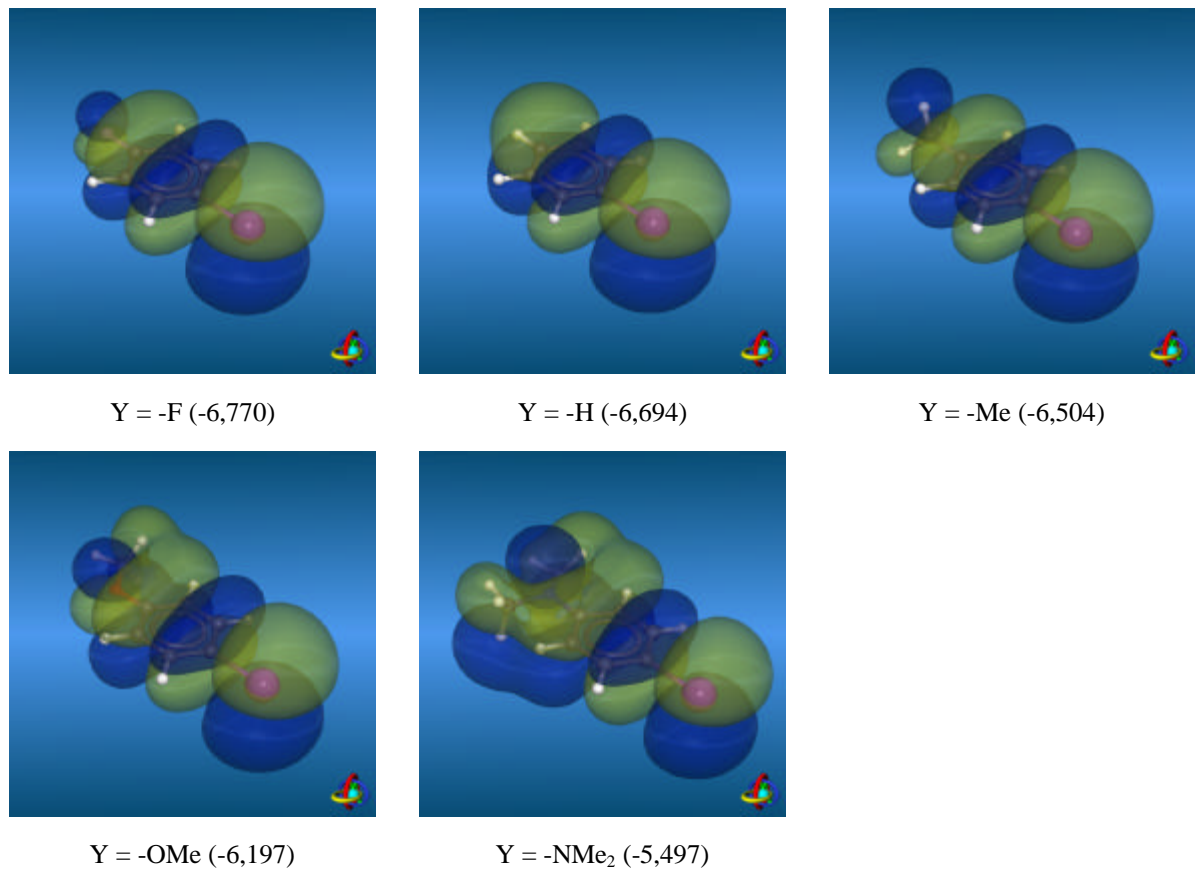


Fig. 7. Highest occupied Kohn-Sham orbitals (HOMOs, B3LYP/6-311++G(d,p) with LANL2DZ ECP on Br, 99% probability contour plots with yellow and blue colors indicating opposite sign of the wave function, all energies in eV) for *para*-substituted iodo-benzenes ($X = \text{-I}$). Note that for $Y = \text{-SOMe}$ the HOMO (-6,636eV) mostly represents the free electron pair located at the sulfur atom, and therefore, was replaced by the HOMO-1 (-7,138eV) in the above plots.